JMEPEG (2012) 21:437–449
DOI: 10.1007/s11665-011-9955-7

1059-9495/$19.00

A Concurrent Product-Development Approach for Friction-Stir Welded Vehicle-Underbody Structures

M. Grujicic, G. Arakere, A. Hariharan, and B. Pandurangan

(Submitted March 19, 2011)

High-strength aluminum and titanium alloys with superior blast/ballistic resistance against armor piercing (AP) threats and with high vehicle light-weighing potential are being increasingly used as military-vehicle armor. Due to the complex structure of these vehicles, they are commonly constructed through joining (mainly welding) of the individual components. Unfortunately, these alloys are not very amenable to conventional fusion-based welding technologies [e.g., gas metal arc welding (GMAW)] and to obtain high-quality welds, solid-state joining technologies such as friction-stir welding (FSW) have to be employed. However, since FSW is a relatively new and fairly complex joining technology, its introduction into advanced military-vehicle-underbody structures is not straight forward and entails a comprehensive multi-prong approach which addresses concurrently and interactively all the aspects associated with the components/vehicle-underbody design, fabrication, and testing. One such approach is developed and applied in this study. The approach consists of a number of well-defined steps taking place concurrently and relies on two-way interactions between various steps. The approach is critically assessed using a strengths, weaknesses, opportunities, and threats (SWOT) analysis.

Keywords blast-survivable and ballistic threat-resistant military vehicles, friction-stir welding, process development

1. Introduction

Friction-stir welding (FSW) is a solid-state metal-joining process (Ref 1). The basic concept behind FSW is described using the example of flat-butt weld, Fig. 1. As shown in Fig. 1, a non-consumable rotating tool moves along the contacting surfaces of two rigidly butt-clamped plates. As seen in this figure, the tool consists of a threaded conical pin with four flutes. During welding, the workpiece (i.e., the two clamped plates) is placed on a rigid backing support, the shoulder is forced to make a firm contact with the top surface of the workpiece while the tool is rotated and advanced along the butting surfaces. Due to frictional sliding, heat is generated at the shoulder/workpiece and at the pin/workpiece contact surfaces. This, in turn, causes an increase in the workpiece/tool temperature and gives rise to pronounced softening of the workpiece material adjacent to these contacting surfaces. As the tool advances along the butting surfaces, thermally softened workpiece material in front of the tool is back-extruded around the tool, stirred/heavily deformed (this process also generates heat), and ultimately compacted/forged into the tool-wake region to form a joint/weld.

M. Grujicic, G. Arakere, A. Hariharan, and **B. Pandurangan**, Department of Mechanical Engineering, Clemson University, 241 Engineering Innovation Building, Clemson, SC 29634-0921. Contact e-mail: gmica@clemson.edu.

Relative to the traditional fusion-welding technologies such as gas metal arc welding (GMAW), FSW offers a number of advantages. Unfortunately, there are also several potential challenges associated with the use of FSW. Since a detailed discussion pertaining to the main advantages and shortcomings of FSW was presented in our prior study (Ref 2-7), only a summary of these is provided in Table 1.

FSW has established itself as a preferred joining technique for aluminum components and its applications for joining other *difficult-to-weld* metals (e.g., titanium-based alloys) is gradually expanding. Currently, FSW is being widely used in many industrial sectors such as shipbuilding and marine, aerospace, railway, land transportation, etc. This joining technology is, in principle, suitable for the fabrication of the welds of different topologies such as: 90° corner, flat-butt, lap, T, spot, fillet, and hem joints, as well as to weld hollow objects, such as tanks and tubes/pipes, stock with different thicknesses, tapered sections, and parts with three-dimensional contours. A collage of the most frequently encountered FSW joints is provided in Fig. 2.

In order to respond to the new enemy threats and warfare tactics, military systems, in particular, those supporting the U.S. ground forces, are being continuously transformed to become faster, more agile, and more mobile so that they can be quickly transported to operations conducted throughout the world. Consequently, an increased emphasis is being placed on the development of improved lightweight body-armor and light-weight vehicle-armor systems as well as on the development of new high-performance armor materials/structures. Therefore, a number of research and development programs are under way to engineer light-weight, highly mobile, transportable, and lethal battlefield vehicles with a target weight under 20 tons. To attain these goals, significant advances are needed in the areas of light-weight structural- and armor-materials development (including aluminum- and titanium-based structural/armor-grade materials). Due to the complex structure of the

military battle-field and tactical vehicle underbodies, the use of aluminum- and titanium-alloy components generally requires component joining by welding. Unfortunately, the high-performance aluminum and titanium alloy grades used in vehicle-armor applications are normally not very amenable to conventional fusion-based welding technologies with the weld-zone and/or heat-affected zone mechanical (and often corrosion) properties being quite deficient in comparison to those found in the base-metal.

In principle, many problems associated with fusion welding of the advanced high-strength aluminum and titanium alloys used in military-vehicle applications can be overcome through the use of FSW. However, since FSW is a relatively new and fairly complex joining technology, its introduction into advanced military-vehicle structures is not straight forward and entails a comprehensive multi-prong approach. Development and application of one such approach is the subject of this study. As will be presented in the next section, the present approach requires concurrent and interactive considerations of the key aspects associated with the components/vehicle design/manufacturing and testing. Since blast-survivability and ballistic resistance (destructive) testing of full-size military-vehicle underbodies is quite costly and time consuming, it is commonly replaced with the corresponding fabrication/testing of sub-scale (look-alike) test structures. Consequently, within this study attention will be given to the fabrication and testing of such sub-scale structures and not to the full-scale vehicle-underbodies.

To critically assess the potential of the proposed approach, the so-called SWOT (strength, weaknesses, opportunities, and threats) analysis is employed. For a well-defined goal/objective, this analysis (frequently used in projects and business ventures) allows for the identification of the internal and external factors that are favorable and unfavorable with respect to the attainment of the goal. The key objective of this study is to develop a computational approach which will enable the low-cost, short lead-time development of blast-resistant vehicle underbodies.

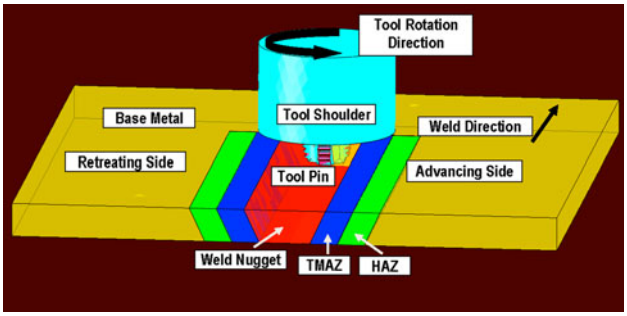

Fig. 1 A schematic of the friction-stir welding (FSW) process used to fabricate a flat-butt joint. Four typical microstructural zones associated with the FSW process are also labeled

Table 1 Main advantages and short-comings associated with the friction-stir welding technology

Advantages	Shortcomings
Good as-weld mechanical properties and joint quality even in alloys unweldable by conventional techniques	An exit hole is left after the tool is withdrawn from the workpiece
Improved safety due to the absence of toxic fumes or the spatter of molten material	Relatively large tool press-down and plates-clamping forces required
No consumables such as the filler metal or gas shield are required	Lower flexibility of the process with respect to variable-thickness and non-linear welds
Ease of process automation	Lower welding rates than conventional fusion-welding techniques. This shortcoming is somewhat lessened since fewer welding passes are required
Ability to operate in horizontal, vertical, overhead, and orbital positions as there is no weld pool	It is a relatively costly process
Minimal thickness under/over-matching which reduces the need for expensive post-weld machining	
Low environmental impact	
Ability to produce aluminum-alloy welds in a 0.02-3.0 in range in a single pass	
Dissimilar aluminum-alloy grades can be readily FSWed (e.g., AA6061 to AA5083, wrought and cast aluminum alloys as well as aluminum matrix composites)	
Substantially lower attendant temperatures, residual stresses and distortions in comparison to those encountered in traditional arc welding processes	
Superior impact resistance property of the FSW joint due to a fine equiaxed grain structure in the innermost zone	
Complete absence of filler-induced defects (no fillers used) and hydrogen-embrittlement cracking (no hydrocarbon fuel used)	
Conventional milling machines can be converted into FSW machines	
Fastened joints can be replaced of with FSW joints leading to significant savings in weight reduction and cost	
Difficult to join 2xxx and 7xxx aluminum alloys can be joined by FSW without any solidification-induced defects	
Particularly suited for butt and lap joining of difficult-to-join aluminum alloys	

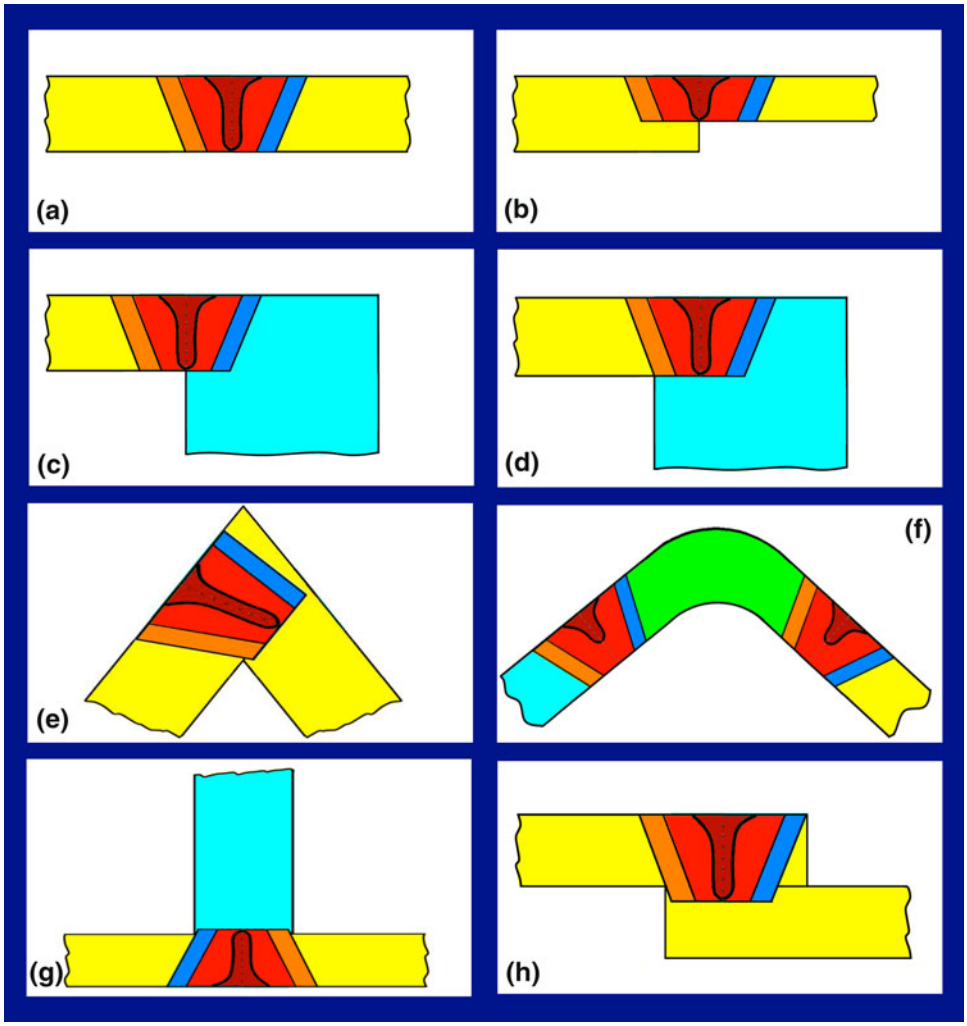

Fig. 2 Typical joint/weld geometries/designs fabricated using the FSW process: (a) flat-butt joint; (b) unequal thickness flat-butt joint; (c) 90° corner-butt joint; (d) 90° corner rabbeted joint; (e) angle joint; (f) transition weld joint; (g) T-joint; and (h) lap joint

2. Concurrent Vehicle-Underbody Design, Fabrication, and Testing

Design, manufacturing, and blast-survivability performance testing of military-vehicle-underbody sub-scale test structures is a highly complex and time-consuming process. It is generally recognized that the lead-time and the cost of this process can be greatly reduced by addressing the issues related to designing, manufacturing, and testing concurrently and interactively. In this section, a new fully integrated approach for the concurrent design, FSW-based manufacturing, and testing of high-survivability military-vehicle underbodies is introduced. As will be seen, while this approach contains a number of discrete steps, these steps are most often carried out concurrently and multiple iterations/interactions between different steps are encountered. To help understanding of the proposed approach, a flowchart is provided in Fig. 3. As seen in this figure, the main steps encountered in the present approach include:

2.1 Step 1: Preliminary/Modified Design

Within this step, legacy knowledge related to the performance of the vehicles during combat operations or field testing are combined with the results of preliminary studies pertaining to blast-survivability of different FSW joint configurations and the design for manufacturing principles, to arrive at a preliminary (and, subsequently modified) design. All three (conceptual, embodiment, and detailed) design stages are included and the topological (e.g., flat-butt, 90° corner butt, etc.) and geometrical (e.g., linearity, depth, etc.) details related to different FSW joints are identified and passed to the next step.

2.2 Step 2: FSW Process Modeling

Within this step, input FSW weld topologies and geometries from step 1 are combined with FSW process parameters (e.g., tool geometry, tool material, tool rotational and travel speeds, etc.), legacy knowledge and the results of preliminary tests pertaining to the correlation between FSW process parameters and the weld microstructure/properties. These are next used within a FSW process model (e.g., 2-7) to determine spatial distribution of the workpiece material microstructure (as well as properties and residual stresses) within different weld zones (i.e., weld-nugget, thermo-mechanically affected zone, and heat-affected zone).

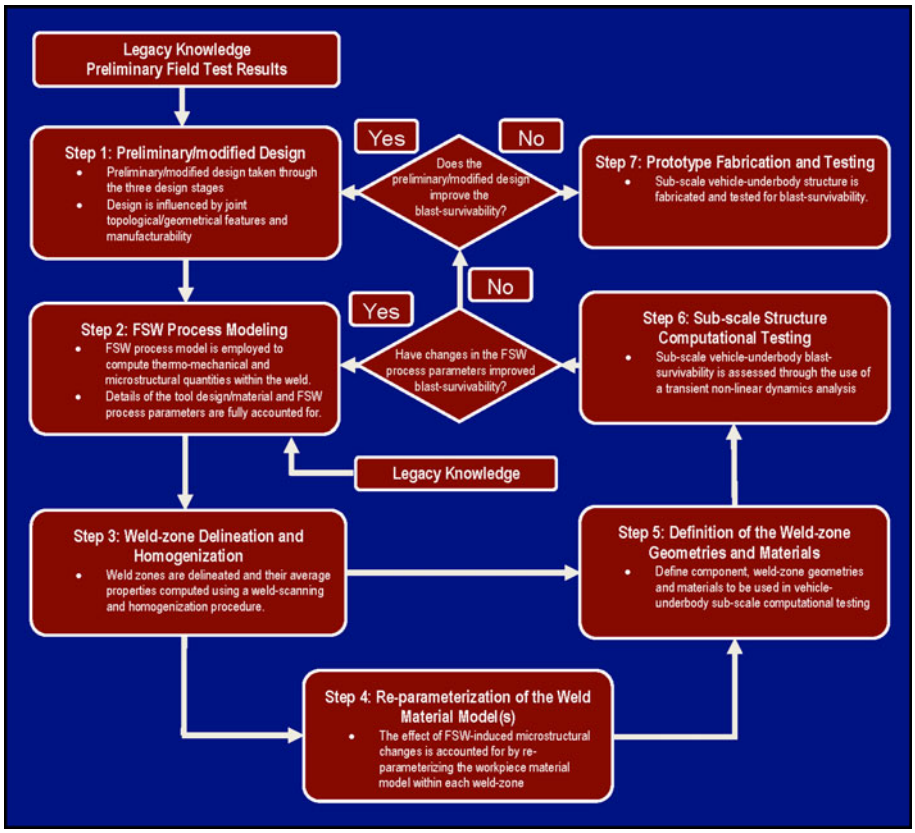

Fig. 3 A flow chart of the proposed concurrent design, manufacturing, and testing approach

2.3 Step 3: Weld-Zone Delineation and Homogenization

The results obtained in step 2 are used within a weld-scanning and homogenization procedure to delineate the boundaries between the different weld zones and to compute the average values of the microstructural parameters (e.g., grain-size, degree of recrystallization, equivalent plastic strain, etc.) within each zone.

2.4 Step 4: Re-Parameterization of the Weld-Material Model(s)

Within this step, average values of the microstructural parameters for each of the weld zones, as obtained in step 3, are used to appropriately adjust the corresponding material model parameters relative to their base-metal counterparts to include the effect of FSW-induced changes in the material microstructure and properties within each zone. This is a very critical step and typically its success depends on the availability and the quality of the open literature, legacy, and proprietary results relating the microstructure and properties of the materials in question.

2.5 Step 5: Definition of the Weld-Zone Geometries and Materials

The results obtained in step 3 which pertain to the geometry of different weld zones are combined with the material model re-parameterization results obtained in step 4, and used to define the components and joints geometries and materials as needed in a transient non-linear dynamics analysis of blast loaded sub-scale test structures.

2.6 Step 6: Sub-Scale Test-Structure Survivability

The designs obtained in steps 1 and 5 are pre-processed (e.g., meshed, fixtured, etc.) and subjected to blast loading within a transient non-linear dynamics analysis and the results obtained used to quantify vehicle-underbody sub-scale test-structure survivability.

2.6.1 Inner-Loop: FSW Process/Structure Testing Iterations. While keeping the preliminary design obtained in step 1 unchanged, FSW process parameters are systematically varied within an optimization scheme to maximize vehicle-underbody sub-scale test-structure blast-survivability.

2.6.2 Outer-Loop: Preliminary-Design Modifications. The results obtained in the previous steps are utilized collectively to identify potential modifications in the preliminary design and the process is continued starting with step 2. Modifications in the design are carried out until further design changes do not any longer appreciably affect the blast-survivability of the sub-scale test structure.

At this point, the design is "*frozen*".

2.7 Step 7: Test-Structure Fabrication and Testing

Following the final design obtained within the outer iteration loop, the sub-scale test structure is fabricated and tested for blast/ballistic-impact survivability to provide the proof of concept.

Each of the aforementioned steps is associated with a consideration of important design, manufacturing, and testing aspects as related to the vehicle-underbody sub-scale test structures. The most important of these aspects which were not

considered in our prior study (Ref 2-7) are analyzed in the remainder of this manuscript.

3. Step 1

As stated earlier, within this step, legacy knowledge is combined with the results of preliminary studies pertaining to blast-survivability of different FSW joint configurations and the design for manufacturing principles, to arrive at a preliminary (and, subsequently modified) vehicle-underbody design. When designing the test structures, it is critical to ensure that their topology and design (e.g., plates, stiffeners, and structural details) closely resemble those of a prototypical military vehicle so that the results obtained can be used to judge blast-survivability of the vehicle structures themselves. An example of the (sub-scale) vehicle-underbody structure is displayed in Fig. 4. The main issues related to the use of legacy knowledge and preliminary test results have been discussed in our recent study (Ref 5). In the remainder of this section, a brief discussion is provided regarding the main issues related to the consideration of test-structure manufacturability within the design step.

As discussed earlier, the manufacturing of advanced military-vehicle-underbody structures capable of enduring ballistic/blast forces involves the utilization of friction-stir welding (FSW) (to join the vehicle components). In general, manufacturability of the FSW weldments in question needs to be considered during the design phase of the component(s) and the vehicle. This approach, commonly referred to as "design for manufacturing" (DFM), is an economically attractive option since it may greatly reduce refabricating/retrofitting costs and mainly involves the conceptual and the embodiment design stages (the stages which are associated with the lowest product-development cost). In the remainder of this section, examples are provided of the most frequently encountered aspects of DFM within the context of FSW of high-survivability military-vehicle-underbody structures.

3.1 Weld-Region Accessibility to the FSW Tool

A typical FSW-tool assembly consists of a circular-cylindrical flat shoulder and a pin. This tool assembly is mounted on a tool holder (also referred to as the shank) which is connected to the machine spindle. The machine spindle itself is connected to the load cell and the load cell housing making the entire tool/tool-holder assembly quite bulky. The bulky nature of the FSW-tool/tool holder assembly may lead to inaccessibility of the weld region to the FSW tool. An example of the case in which the initial design may not be adequate with respect to the weld-region accessibility to the FSW tool is depicted in Fig. 5(a). A modified design in which the problem of weld-region accessibility is corrected is provided in Fig. 5(b). An alternative modified design in which the length of the horizontal member is increased is provided in Fig. 5(c). It should be noted that the modified design(s), may, in general compromise the functional performance of the weldment or reduce its mass efficiency. Consequently, both the weld-region accessibility to the tool and the component functional performance/mass efficiency have to be considered concurrently.

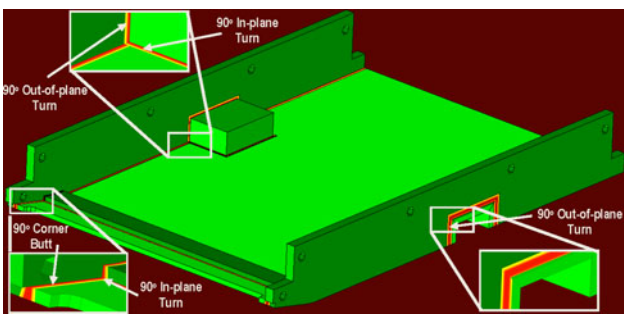

Fig. 4 An example of the (sub-scale) vehicle-underbody structure

3.2 Weld-Joint Design/Configuration

The design of military-vehicle structures involves the selection of appropriate weld-joint designs (e.g., butt, lap, T-joint, etc.) in different sections of the vehicle. While, all these joint designs can be manufactured using FSW, flat, and 90° corner-butt joints have been demonstrated to be most easily fabricated, and to yield superior static and ballistic/blast strength performance (where the latter strength performance is typically assessed using the so-called ballistic shock test procedure, Ref 8). Consequently, designs involving the use of butt joints are generally preferred. For example, a T-joint, displayed in Fig. 6(a), of high quality is quite challenging to produce using FSW. As shown in Fig. 6(b), a T-joint may be replaced by a pair of more easily manufacturable 90° corner-butt joints.

3.3 Component Fixturing for FSW

The FSW process requires the use of stiff and strong fixtures to: (a) ensure large contact pressures along the butting surfaces;

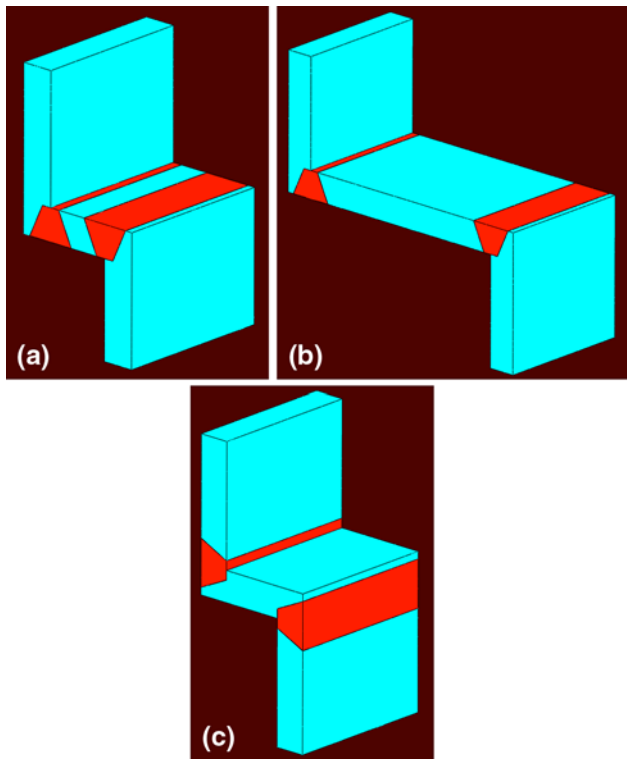

Fig. 5 (a) Original weldment design which may be difficult to fabricate due to lack of weld-region accessibility by the FSW tool; (b, c) two potential modified designs

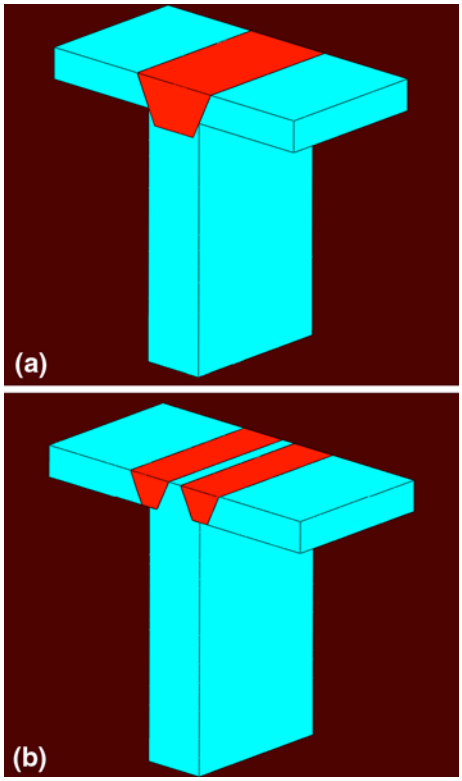

Fig. 6 (a) Original weldment design containing a single T-joint which may require multi-pass FSW procedure; and (b) a potential modified design containing two 90° corner-butt joints

and (b) prevent welding component deflection and displacement during the welding process. In general, strict fixturing requirements must be met to produce good-quality FSW joints. Meeting these fixturing requirements may become challenging due to the inherent shape of the welding components as well as the location of the welds. An example of the two FSW-joint weldments in which fixturing may become important is displayed in Fig. 7(a), (b). The design in Fig. 7(a) is associated with geometrically more complex fixtures and with the need for the application of clamping forces in non-orthogonal directions. In addition, the shape of two out of three components is relatively complex. In the modified design in Fig. 7(b), only geometrically simple and orthogonal fixturing is needed and the component's shape is simplified. An examination of Fig. 7(b) shows that the revised design may be deficient with respect to meeting the weld-region accessibility requirements. Thus, during the components/structure design stage, all the critical FSW-based DFM aspects must be considered.

4. Step 2

As stated earlier, within this step, input FSW weld topologies and geometries from step 1 are combined with FSW process parameters, legacy knowledge, and the results of preliminary tests and used within a FSW process model to determine spatial distribution of the workpiece material microstructure (and properties) within different weld zones. In the remainder of this section, a brief description is provided regarding the structure of a typical FSW process model. Since

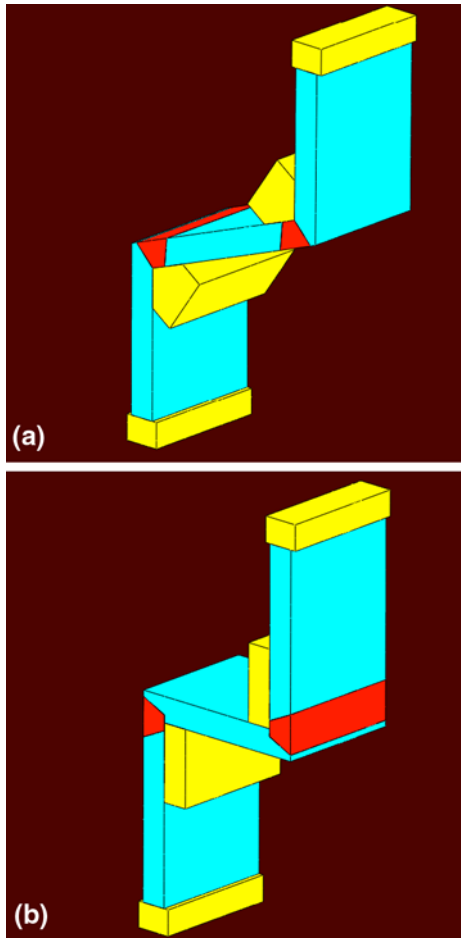

Fig. 7 (a) Original weldment design requiring complex fixturing and non-orthogonal clamping forces; and (b) a modified design requiring simple fixturing, orthogonal clamping, and geometrically simpler components

the FSW-tool design and tool material are important FSW process-model input parameters, and they were not considered in our prior study, they will also be briefly overviewed in this section.

4.1 FSW Process Modeling

FSW normally involves complex interactions and competition between various thermo-mechanical processes such as frictional-energy dissipation, plastic deformation, and the associated heat dissipation, material transport/flow, material microstructure evolution (e.g., grain-growth, precipitate coarsening, recrystallization, etc.), and local cooling (Ref 8-15). A unique feature of the FSW process is that heat transfer does not only take place via thermal conduction but also via transport of the workpiece material adjacent to the tool from the region in front to the region behind the advancing tool. In general, both the heat- and the mass-transfer depend on the workpiece material properties, tool geometry, and the FSW process parameters. Mass transport during FSW is accompanied by extensive plastic deformation (with maximum equivalent plastic strains of the order of 10-50) of the transported material with the attendant strain rates as high as 10 s^{-1} (Ref 16, 17).

Over the last 10-15 years, considerable effort has been expended toward developing computational methods and tools

for analyzing the FSW joining process, quality of the resulting weld as well as the microstructure and properties of the workpiece material in the as-welded state. A detailed overview of the existing FSW process models was presented in our prior work (Ref 2, 3). Hence, no similar in-depth overview will be presented here. Instead, only the aspects of a typical FSW process model which are pertinent to the present concurrent design, fabrication, and testing approach will be discussed.

A typical FSW process model requires specification of a number of input parameters such as the workpiece material properties, component's geometry, weld topology, and FSW process parameters. The main FSW process parameters include: (a) tool-design/material; (b) rotational and translational velocities of the tool; (c) tool-plunge depth; (d) tool tilt-angle; and (e) tool-dwell time (the FSW process typically involves three distinct stages: (a) tool plunging; (b) dwelling; and (c) welding).

Within a typical FSW process model, the mass, momentum, and energy conservation equations are solved under the conditions specified by the aforementioned input parameters to determine the associated thermo-mechanical fields (e.g., temperature, equivalent plastic strain, equivalent plastic strain rate, stress components, particle velocities, etc.). The model is frequently combined with a microstructure material model. In this case, the list of field quantities includes additional (microstructural) parameters such as grain-size, the extent of precipitate coarsening, degree of recrystallization, etc. An example of the latter type of FSW process model can be found in our recent study, e.g. (Ref 3, 4), in which a fully coupled thermo-mechanical finite-element analysis is employed to solve the governing mass, momentum and heat-transfer conservation equations combined with the microstructure-evolution equations (describing the basic physical metallurgy of the aluminum alloy grades being FSWed). Within this model, various microstructure-evolution processes taking place during FSW (e.g., extensive plastic-deformation-induced grain-shape distortion and dislocation-density increase, dynamic recrystallization, and precipitates coarsening, over-aging, dissolution and re-precipitation) are considered to predict the material microstructure/properties in the various FSW zones of the alloys being welded. For each of the aforementioned microstructure-evolution processes, the appropriate material state variables are introduced and their evolution equations constructed and parameterized (using available open literature sources pertaining to the kinetics of the microstructure-evolution processes). Next, the thermo-mechanical constitutive models for the alloys being FSWed are modified to include the effect of the local material microstructure on the material response during FSW. This approach enabled examination of the two-way interactions between the FSW process and the weld-material microstructure evolution. In other words, both the effect of the current material microstructure on its thermo-mechanical response during the FSW process and the effects of thermo-mechanical history of a material point during the FSW process on the associated microstructure are analyzed.

4.2 FSW-Tool Design/Material

4.2.1 Tool Design. Tool design is one of the most important factors that influences the FSW joint quality as well as the weld-material microstructure and properties. A typical FSW tool, in its base-line configuration, consists of two main sections, a solid right circular-cylindrical (RCC) shoulder and a solid RCC pin. Both the shoulder and the pin play an important role in the FSW process, affecting heat generation, material-flow, weld quality as well as the power required for welding. The tool shoulder is responsible for the majority of heat generation via frictional sliding at the tool-shoulder/workpiece interface, while both the tool shoulder and the pin affect the material-flow/stirring and the weld quality. It is generally recognized that the base-line FSW-tool design produces limited material-flow and mixing. Consequently, in recent years several tool designs were proposed which improve the efficiency of the FSW process and the resulting weld quality over the ones obtained using the base-line design. These new tools typically contain modified designs in both the shoulder and the pin sections. The two main modifications in the FSW-tool shoulder are: (a) concave shoulder profile; and (b) flat shoulder with scrolls. These modifications are displayed and labeled in Fig. 7(a), (b) and their use is found to greatly enhance material stirring and deformation and typically results in joints of improved quality. Additionally, the concave shoulder profile reduces workpiece/weld thickness mismatch while scrolls eliminate the need for tool-tilting and, thus, promote the fabrication of non-linear (e.g., 90° turn flat-butt) welds.

The main FSW-tool pin modifications include: (a) non-flat bottom (lowers the wear-rate and tendency for fracture at the expense of material stirring extent); (b) taper (lowers the longitudinal loads experienced by the pin); (c) threads (promotes material mixing in the workpiece thickness direction and improves material forging in the same direction); (d) stepped spiral (performs a role similar to threads); and (d) flats and flutes (enhances the extent of material stirring, plastic deformation, and thermal softening which, in turn, enables higher welding speeds). These pin-design modifications are also displayed and labeled in Fig. 8(a) to (c).

The nature and the extent of modifications of the FSW-tool base-line design is controlled by a number of factors such as: (a) the workpiece material (e.g., in the case of FSW of high-temperature materials, stepped-spirals are more frequently used than threads since the latter are prone to wear and fracture) and tool materials (e.g., threads/stepped-spirals are difficult to machine in low-ductility ceramic materials and these features may result in pronounced stress concentration effects); (b) the weld-joint design (e.g., in the case of lap joints, tools with two shoulders are often used. The lower shoulder is smaller in diameter and is plunged down to the joint interface while the top shoulder (larger diameter) rests on the top surface of the workpiece); (c) FSW process parameters (e.g., features which promote extensive heat generation and material softening via frictional sliding and material stirring/plastic deformation are used when larger welding speeds are desired); and (d) manufacturer's prior experience (i.e., legacy and proprietary knowledge regarding the suitability of different tool designs for different FSW applications is still a major factor controlling the design of the FSW tool).

4.2.2 Tool Materials. Friction-stir welding (FSW) is a thermo-mechanical deformation process during which the tool temperature approaches the workpiece solidus temperature (the minimum temperature at which the liquid phase is observed during heating) and the tool is subjected to large normal and shear contact stresses. In order to produce good-quality welds for a particular application, not only the appropriate tool design but also the selection of the appropriate tool material is critical. The selection of FSW-tool materials is guided by the fulfillment of the functional requirements such as: (a) long service-life as governed by wear, fracture, workpiece/tool chemical-interactions, and thermal-decomposition processes; (b) availability and

cost; and (c) good dimensional stability under high-temperature working conditions. By employing the conventional material selection principles (Ref 18), the following thermo-mechano-physical properties are identified as being the most critical in the case of FSW tools: (a) strength at elevated as well as ambient temperatures; (b) thermal and chemical stability at elevated-temperatures; (c) wear resistance; (d) workpiece/tool chemical reactivity; (e) material fracture toughness; (f) coefficient of thermal expansion (in the case of multi-material tools); (g) machinability; and (h) uniformity in microstructure, density, and property distributions (primarily in the case of powder metallurgy fabricated FSW tools). While, ranking of these material properties may be highly subjective, the order in which the properties are listed above is consistent with the most commonly used FSW-tool material property ranking.

The tool materials most commonly used in the FSW-tool applications are as follows: (a) tool steels (e.g., AISI H13); (b) nickel- and cobalt-base alloys (e.g., Inconel738LC and MP 159); (c) refractory metals (e.g., tungsten, molybdenum, niobium, and tantalum); (d) crystalline ceramics [e.g., carbides like titanium carbide and polycrystalline cubic-boron nitride (PCBN)]; and (e) metal-matrix composites (e.g., W + 1vol.%La_2O_3, W-Re + 2vol.%HfC). A summary of the common FSW-tool materials and the critical material properties is provided in Table 2, in this table, materials performance with respect to the properties in question is ranked using an excellent/good/fair/poor scale.

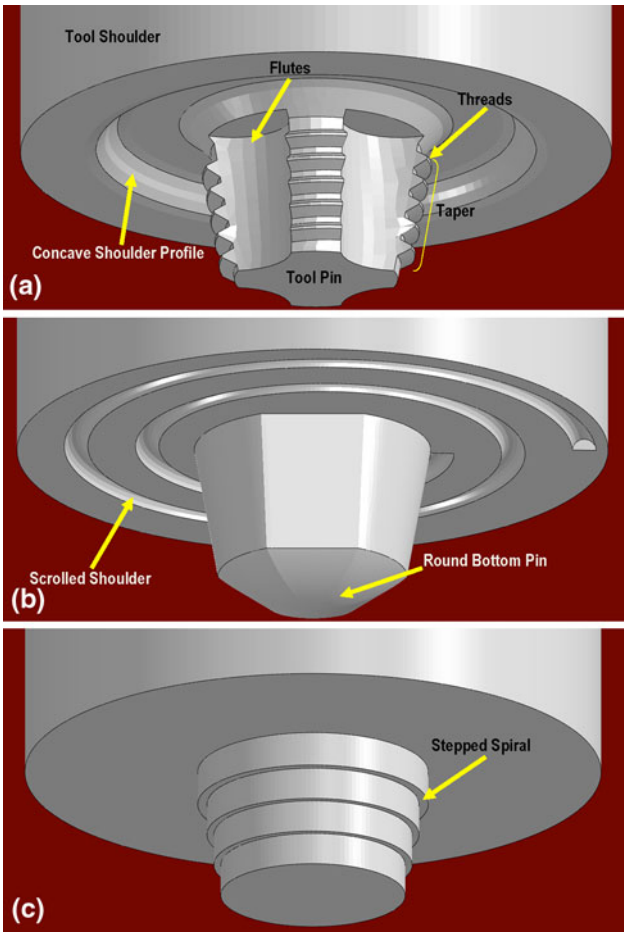

Fig. 8 FSW-tool pin-design modifications

5. Step 3

As discussed earlier, the application of a typical FSW process model produces a number of thermo-mechanical fields (e.g., temperature, equivalent plastic strain, equivalent plastic strain rate, residual stress components, particle velocities, etc.) associated with the formation of the FSW joint in question. In addition, such a model may produce a number of microstructural fields (e.g., grain-size, the extent of precipitate coarsening, degree of recrystallization, etc.) in the final joint. Here, the latter fields can be used to define the boundaries between the base-metal and the weld as well as to define the boundary between different zones of the weld. Typically, a FSW weldment contains four distinct microstructural zones:

(a) a base-metal zone which is far enough from the weld so that material microstructure/properties are not altered by the joining process;
(b) the heat-affected zone (HAZ) in which material microstructure/properties are affected only by the thermal effects associated with FSW. While this zone is normally found in the case of fusion-welds, the nature of the microstructural changes may be different in the FSW case due to generally lower temperatures and a more diffuse heat source;
(c) the thermo-mechanically affected zone (TMAZ) which is located closer than the HAZ zone to the butting surfaces. Consequently, both the thermal and the mechanical aspects of the FSW affect the material microstructure/properties in this zone. Typically, the

Table 2 Common FSW-tool materials and their critical properties

Material	Property				
	High-temperature strength	Wear resistance	Fracture toughness	Machinability	High-temperature chemical stability
Tool steels (e.g., AISI H13, high-speed grades)	Good	Good	Good-to-excellent	Excellent	Good
Ni-Co-based alloys (e.g., Inconel738LC and MP 159)	Good	Good	Good-to-excellent	Good-to-excellent	Good
Refractory metals (e.g., W, W-Re, Mo, Nb, Ta)	Excellent	Good	Fair-to-poor	Poor	Fair
Crystalline ceramics (e.g., TiC, PCBN, WC)	Good-to-excellent	Good-to-excellent	Fair-to-poor	Poor	Excellent
Metal matrix composites (e.g., W + 1vol.%La_2O_3, W-Re + 2vol.%HfC)	Excellent	Excellent	Good	Fair	Fair-to-good

original grains are retained in this zone although they may have undergone severe plastic deformation; and

(d) the weld-*nugget* is the innermost zone of an FSW joint. As a result of the way the material is transported from the regions ahead of the tool to the wake regions behind the tool, this zone typically contains the so-called onion-ring features. The material in this region has been subjected to most severe conditions of plastic deformation and high-temperature exposure and consequently contains a very-fine dynamically recrystallized equiaxed grain microstructure.

Before one can define the boundaries between the four microstructural zones, the key thermo-mechanical and microstructural parameter(s) for the alloy in question must be identified. For example, aluminum alloys can be broadly classified as non-heat-treatable (non-age-hardenable) and heat-treatable (age/precipitate hardenable) aluminum alloys. In the case of non-heat-treatable aluminum alloys, material strength and ductility is mainly controlled by the grain-size and the extent of strain hardening (as defined by the competition between plastic deformation and dynamic recrystallization). Thus, the main parameters used to delineate different microstructural zones are, in this case, the grain-size, the equivalent plastic strain, and the degree of recrystallization. In the case of heat-treatable alloys, on the other hand, as-welded material mechanical properties are mainly controlled by age or precipitate hardening. Hence, the key microstructural parameters include the extent of precipitate over-aging/dissolution as well as the ones mentioned in the context of non-heat-treatable alloys.

Another critical step in the weld-zone delineation process is the definition of the threshold values for the parameters identified above. This is important since the thermo-mechanical and microstructural fields are generally smooth and the use of such threshold values helps decision making regarding the position of the inter-zone boundaries. For example, one must define the minimal (threshold) increase in the local grain-size at a material point, relative to that in the base-metal zone, for the point to be considered a part of the *HAZ*. Similarly, a minimal threshold value for the degree of recrystallization must be defined for the definition of the *TMAZ*/weld-nugget boundary.

Once the key microstructural parameters are identified and the threshold values selected, a simple microstructure scanning algorithm can be utilized to delineate the four microstructural zones. This is demonstrated in Fig. 9(a) to (e).

Figure 9(a), (b), and (c) shows examples of the field plots pertaining, respectively, to the grain-size, equivalent plastic strain, and the degree of recrystallization distributions over a transverse section of the single flat-butt joint weldment. A fine quadrilateral grid, Fig. 9(d), is placed over the field plots and combined with the grain-size, equivalent plastic strain, and the degree of recrystallization threshold values to define the boundaries between the four microstructural zones, Fig. 9(e). In Fig. 9(e), the base-metal/HAZ boundary is defined by a 61.2 μm grain-size contour (a 20% increase relative to the base-metal grain-size), the HAZ/TMAZ boundary by a 0.3 equivalent plastic strain contour, while the TMAZ/weld-nugget boundary is defined by a 0.7 degree of recrystallization contour line.

Once the HAZ, TMAZ, and the weld-nugget are defined, one can calculate an average value of the thermo-mechanical and microstructural parameters within each of these three zones. Following the procedure described in the next section, these average values are next used to re-parameterize the workpiece material model within each of the weld zones.

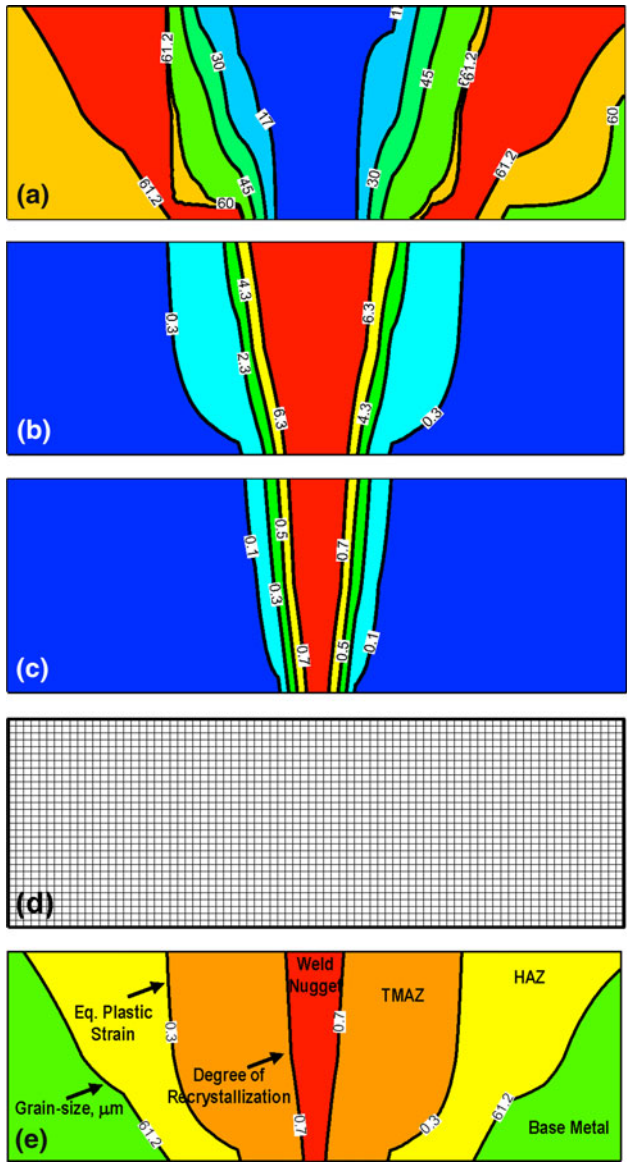

Fig. 9 Typical distributions of the: (a) grain-size; (b) equivalent plastic strain; (c) degree of recrystallization over a transverse section of a flat-butt FSW weld; (d) the grid used for identification of weld inter-zone boundaries; and (e) the resulting weld decomposition into three distinct zones

6. Step 4

As discussed earlier, within this step, average values of the microstructural parameters for each of the weld zones, as obtained in step 3, are used to appropriately adjust the corresponding material model parameters relative to their base-metal counterparts to include the effect of FSW-induced changes in the material microstructure and properties within each zone. While there is a relatively large selection of material models that can be used to describe the mechanical behavior of metallic systems, the Johnson-Cook deformation and fracture model (Ref 19, 20) are most frequently used. This model is capable of representing the material behavior displayed under

large-strain, high deformation rate, high-temperature conditions, of the type encountered in the problem of computational modeling of both the FSW process and the ballistic/blast loading of a vehicle sub-scale test structure. Deformation and failure components of this model are briefly reviewed below.

6.1 Deformation

Within this model, the (workpiece) material is considered as being an isotropic linear-elastic and a strain-rate sensitive, strain-hardenable, and (reversibly) thermally softenable plastic. The deformation response of the material is defined using the following three relations: (a) a *yield criterion*, i.e., a mathematical relation which defines the condition which must be satisfied for the onset (and continuation) of plastic deformation; (b) a *flow rule*, i.e., a relation which describes the rate of change of different plastic strain components during plastic deformation; and (c) a *constitutive law*, i.e., a relation which describes how the material strength changes as a function of the extent of plastic deformation, the rate of deformation and temperature. For most aluminum and titanium alloy grades used in military-vehicle FSWed structures, a von Misses yield criterion and a normality flow-rule are used. The von Misses yield criterion states that equivalent stress must be equal to the material yield strength for plastic deformation to occur. The normality flow-rule states that the plastic flow takes place in the direction of the stress-gradient of the yield surface (i.e., in a direction normal to the yield surface, when the latter is defined in the stress space). The Johnson-Cook strength constitutive law is defined as:

$$\sigma_y = \left[A + B(\bar{\varepsilon}^{\mathrm{pl}})^n\right]\left[1 + C_1 \log(\dot{\bar{\varepsilon}}^{\mathrm{pl}}/\dot{\bar{\varepsilon}}_o^{\mathrm{pl}})\right]\left[1 - T_H^m\right] \qquad \text{(Eq 1)}$$

where $\bar{\varepsilon}^{\mathrm{pl}}$ is the equivalent plastic strain, $\dot{\bar{\varepsilon}}^{\mathrm{pl}}$ is the equivalent plastic strain rate, $\dot{\bar{\varepsilon}}_o^{\mathrm{pl}}$ is a reference equivalent plastic strain rate, A is the zero-plastic strain, unit-plastic strain rate, room-temperature yield strength, B is the strain-hardening constant, n is the strain- hardening exponent, C_1 is the strain-rate constant, m is the thermal-softening exponent, and $T_H = (T - T_{\mathrm{room}})/(T_{\mathrm{melt}} - T_{\mathrm{room}})$ a room-temperature (T_{room})-based homologous temperature while T_{melt} is the melting temperature. All temperatures are given in Kelvin.

6.2 Failure

Within this model, the material failure is assumed to be of a ductile character and the progress of failure is defined by the following cumulative damage law:

$$D = \sum \frac{\Delta\varepsilon}{\varepsilon_{\mathrm{f}}} \qquad \text{(Eq 2)}$$

where $\Delta\varepsilon$ is the increment in effective plastic strain with an increment in loading and ε_{f} is the failure strain at the current state of loading which is a function of the mean stress, the effective stress, the strain rate, and the homologous temperature, given by:

$$\varepsilon_{\mathrm{f}} = D_1\left[1 + \frac{D_2}{D_1}\exp(-D_3\sigma^*)\right]\left[1 + D_4 \ln \dot{\varepsilon}_{\mathrm{pl}}\right]\left[1 + D_5 T_H\right] \qquad \text{(Eq 3)}$$

where σ^* is mean stress normalized by the effective stress. The parameters D_1, D_2, D_3, D_4, and D_5 are all material-specific constants. Failure is assumed to occur when D as defined in Eq 2 is equal to 1.0.

6.3 Model Re-Parameterization

In a typical situation, the Johnson-Cook model for the workpiece base-metal is available, i.e., the material model parameters A, B, n, etc. are known. The challenge then is to re-parameterize this model for the remaining three microstructural zones to account for the FSW-induced changes in the respective material microstructures. While, in principle, all the Johnson-Cook material model parameters are expected to be microstructure dependent, it is a common practice to identify and re-parameterize only those material model parameters which are most sensitive to the changes in the material microstructure. The two material parameters generally considered to be belonging to this class are A (the initial material yield strength) and D_1 (material ductility, while the D_2/D_1 ratio is kept constant).

Revaluation of the parameter A will, in general, depend on the type of the workpiece material in question. Specifically, in non-heat-treatable alloys changes in the yield strength within the three weld zones are controlled by grain-size and strain-hardening effects, with the grain-size effects being dominant in the HAZ and in the weld-nugget while strain hardening provides a major contribution in the TMAZ. Consequently, parameter A is redefined in this case as

$$A = A_{\mathrm{WZ}}\left(\frac{d_{\mathrm{FSW,WZ}}}{d_{\mathrm{BM}}}\right)^{-\frac{1}{2}} + B\left(\varepsilon^{\mathrm{p}}_{\mathrm{FSW,WZ}} - \varepsilon^{\mathrm{p}}_{\mathrm{Recrystalized,WZ}}\right)^n \qquad \text{(Eq 4)}$$

where subscripts WZ and BM are used to denote weldzone and base-metal, respectively, the first term on the right-hand side accounts for the Hall-Petch-type (Ref 21) grain-size effect while the second term defines the net effect of FSW-induced strain hardening (resulting from the competition between plastic deformation and dynamic recrystallization). The term $\varepsilon^{\mathrm{p}}_{\mathrm{Recrystalized,WZ}}$ denotes the fraction of the FSW-induced plastic strain whose effect on the material strength has been eliminated by dynamic recrystallization. A functional relationship between this quantity and the degree of recrystallization can be found in our prior study (Ref 4).

In the case of heat-treatable workpiece materials in which age or precipitation hardening controls material strength, the A parameter is redefined as:

$$A = A_{\mathrm{WZ}}\left(\frac{l_{\mathrm{BM}}}{l_{\mathrm{FSW,WZ}}}\right) + B\left(\varepsilon^{\mathrm{p}}_{\mathrm{FSW,WZ}} - \varepsilon^{\mathrm{p}}_{\mathrm{Recrystalized,WZ}}\right)^n \qquad \text{(Eq 5)}$$

where l denotes inter-precipitate spacing and the first term on the right-hand side is defined using an Orowan-type (Ref 21) equation.

As far as the D_1 parameter is concerned, it is first recognized that it is a measure of material ductility. It is, in general, a more challenging task to establish a correlation between material's ductility and its different microstructural features. It is also generally expected that these correlations will depend on the type of workpiece material and that they will be different in the case of heat-treatable and non-heat-treatable alloys. In the absence of these correlations and through recognition that microstructural changes which improve strength generally degrade material ductility (and vice versa), one can assume that the product of the material's strength and ductility raised to a power (q) is nearly constant within a given alloy grade. Based

on this assumption, parameter A in different weld zones can be calculated as:

$$D_{1,\mathrm{WZ}} = \left(\frac{A_{\mathrm{BM}}}{A_{\mathrm{WZ}}}\right)^{\frac{1}{q}} D_{\mathrm{BM}} \qquad \text{(Eq 6)}$$

It should be noted that Eq 6 may not be valid in the case when the grain-size has a dominant effect on the material strength and ductility since the aforementioned strength/ductility trade-off is usually not observed in this case.

7. Step 5

Within step 1, only the geometries of the components to be welded but not the geometries of the welds (and their zones) were defined. In addition, the weld-zone material properties were not available. These deficiencies are eliminated during this step through the use of weld geometries obtained in step 3 and weld-material properties obtained in step 4. In addition, the computed FSW-induced residual stresses can be used to properly define the initial stress state of all components/welds. The vehicle-underbody test-structure computational model is now ready for use in the subsequent non-linear dynamics computational analysis of its blast/ballistic-impact resistance/survivability.

8. Step 6

The updated and preprocessed (meshed, fixtured, with assigned initial, boundary, loading and contact conditions) design of the vehicle-underbody test structures obtained in step 5 is used next within a transient non-linear dynamics computational analysis to assess its blast/ballistic-impact survivability. Typically, survivability is characterized by the lack of penetration and/or of excessive deflection of the test structure. Details regarding the nature of the governing equations and the auxiliary equations which are solved during a typical analysis are discussed here, as well as, of the mine, soil, and air material models and contact/solution algorithms can be found in our prior study [e.g., 22-24]. An example of the qualitative results obtained in this portion of the study is displayed in Fig. 10. Quantitative details regarding the nature of the results obtained and their interpretation cannot be presented or discussed here due to the sensitive character of the subject matter. It is important to emphasize that the computational analysis utilized in this step must, as closely as possible, match the test-structure geometry, joining, material properties, fixturing for testing, and blast/ballistic-impact test conditions that will be used in step 7 (the test-structure fabrication and testing step).

9. Step 7

Within this step, a sub-scale test structure is fabricated and tested under fairly realistic buried-mine blast loading conditions. The test structure is normally required to meet stringent conditions pertaining to the absence of penetration/fragmentation and a lack of excessive deflections. This is a very critical step and must be carried out appropriately to ensure that the

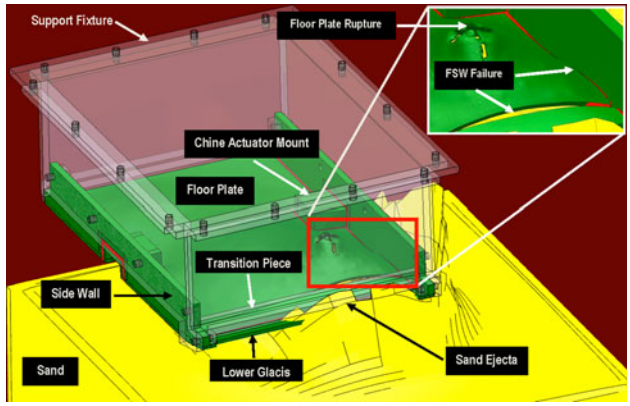

Fig. 10 An example of the computational analysis of blast-survivability of vehicle-underbody structure

results obtained can be used to judge blast-survivability of the vehicle-underbody being developed. Specifically:

(a) The manner in which the test structure is secured to the test fixture and the overall fixture weight should closely resemble their counterparts present in the vehicle. This is a critical requirement since often the performance of structures (including joints) is greatly affected by the effect of surrounding constraints/interactions;
(b) If the test structure is sub-scaled then a dimensional analysis should be employed to account for the scaling effects (e.g., Ref 25);
(c) While a full-factorial blast-testing schedule over the design/test variables (mine size, shape and explosion energy, depth of burial, stand-off distance, soil type, compaction level, degree of saturation, etc.) is preferred, in many cases blast testing under most adverse combinations of these test variables (as suggested by the computational analysis results discussed in step 6) may suffice; and
(d) A comprehensive failure analysis should be conducted following each mine-blast test. Past experience has shown that one can learn a great deal about the behavior of materials and structures by investigating the manner in which they fail in the presence of various loading and constraining conditions.

10. Swot Analysis

As mentioned earlier, SWOT analysis (Ref 26) is a strategic planning or assessment method which identifies internal (strengths and weaknesses) and external (opportunities and threats) factors that are favorable or unfavorable to achieve a given objective. The first step in the SWOT analysis is specification of the desired goal/objective. In this study, the main goal is to develop a fully integrated computation-based analysis, which can be used to speed up and economize the introduction of FSW into the military-vehicle-underbody manufacturing practice.

The next step is to identify the major external and internal factors which may favorably or unfavorably affect the achievement of the desired goal.

Table 3 Results of the SWOT analysis for the proposed concurrent design, manufacturing and testing approach

Strengths	Weaknesses
Modeling and simulation of the FSW process are quite mature	More reliable and physically based models are needed to establish the effect of microstructure on the weld-material strength and ductility
Modeling and simulation of the blast-survivability of the sub-scale vehicle-underbody test structures are also mature	The computational cost associated with the FSW process modeling and simulations and the use of non-rigid detailed design FSW tools can be quite high
Design methodology and optimization techniques are well-established	Issues related to the FSW tool degradation by wear, chemical interaction with the workpiece or thermal decomposition are not currently considered
Data/information regarding the basic metallurgy of many commercially available alloy grades are readily available	
Opportunities	**Threats**
FSW process simulation models are continuously being improved	When new alloy grades are introduced, a relatively long lead time is required before the critical body of knowledge related to basic physical metallurgy is created and made available to the public
Vehicle-underbody test-structure survivability modeling and simulation methods and tools are continuously being improved	When survivability with respect to detonation of buried mines is of concern, reliable physically based model(s) for the soil (at different levels of compaction, clay, gravel and silt moisture contents) are needed. Such models are currently not available in the open literature
New numerical solution algorithms with improved efficiency, stability and robustness are continuously being developed	
Many sources of data/information which are currently of the proprietary nature may become public domain with time	

10.1 Strengths

Strengths are defined as internal/intrinsic factors which play a favorable role in the achievement of the set objective. For example, computational analyses of the FSW process and of the mechanical response of vehicle-underbody structures to blast/ballistic-impact loads are becoming quite mature and hence, their predictions fairly reliable).

10.2 Weaknesses

Weakness is an internal factor which acts unfavorably toward attaining the set goal. For example, prediction of the microstructure evolution (particularly in the case of heat-treatable alloys during FSW) is still far from being mature, yet it plays an important role in obtaining reliable predictions regarding the weld-zone geometries and material properties within the zone.

10.3 Opportunities

These are external factors which may play a favorable role in the attainment of the set goal. For example, in the case of non-heat-treatable alloys, there is a vast source of microstructural/property and hot-working microstructure-evolution data, the conditions encountered during FSW.

10.4 Threats

These are external factors which play an unfavorable role toward the achievement of the goal in question. For example, introduction of newer alloy grades (e.g., AA 2139) whose microstructure/property and hot-working microstructure-evolution data are not either fully defined or available in the open literature, may limit the use of the computational approach proposed in this study.

The results of the application of the SWOT analysis to the previously identified objective are summarized in Table 3. It should be noted that not all the factors appearing in this table are of the same importance. In our future communications, a more refined SWOT analysis will be presented with the proper weights attached to each strength, weakness, opportunity, and threat. It should also be noted that as further progress is made in the analysis of FSW process and more information regarding the material microstructure of the alloys become available in the open literature, weaknesses and threats will become less significant and some will get converted into strengths and opportunities, respectively.

11. Summary

Based on the study presented and discussed in this article, the following main summary remarks and conclusions can be made:

1. A new concurrent approach to designing, manufacturing, and testing of military-vehicle-underbody friction-stir welded structures is proposed.
2. While the proposed approach involves a number of well-defined steps, these steps are highly interactive and often occur concurrently.
3. For each of the steps and their interactions, the key issues are identified and examples of the typical results are presented and discussed.
4. The proposed approach was critically assessed using the so-called SWOT analysis to identify internal and external factors which may favorably or unfavorably affect the success of the proposed approach.

References

1. W.M. Thomas, E.D. Nicholas, J.C. Needham, M.G. Murch, P. Temple-Smith, and C. J. Dawes. Friction Stir Butt Welding, International Patent Application No. PCT/GB92/02203 (1991)
2. M. Grujicic, G. Arakere, H.V. Yalavarthy, T. He, C.-F. Yen, and B.A. Cheeseman, Modeling of AA5083 Material-Microstructure Evolution During Butt Friction-stir Welding, *J. Mater. Eng. Perform.*, 2010, **19**(5), p 672–684

3. M. Grujicic, T. He, G. Arakere, H.V. Yalavarthy, C.-F. Yen, and B.A. Cheeseman, Fully-Coupled Thermo-Mechanical Finite-Element Investigation of Material Evolution During Friction-Stir Welding of AA5083, *J. Eng. Manuf.*, 2010, **224**(4), p 609–625
4. M. Grujicic, G. Arakere, C.-F. Yen, and B.A. Cheeseman, Computational Investigation of Hardness Evolution During Friction-Stir Welding of AA5083 and AA2139 Aluminum Alloys, *J. Mater. Eng. Perform.*, 2010. doi:10.1007/s11665-010-9741-y
5. M. Grujicic, G. Arakere, B. Pandurangan, A. Hariharan, C.-F. Yen, and B.A. Cheeseman, Development of a Robust and Cost-effective Friction Stir Welding Process for Use in Advanced Military Vehicle Structures, *J. Mater. Eng. Perform.*, 2010. doi:10.1007/s11665-010-9650-0
6. M. Grujicic, G. Arakere, B. Pandurangan, A. Hariharan, C.-F. Yen, B.A. Cheeseman, and C. Fountzoulas, Computational Analysis and Experimental Validation of the Ti-6Al-4V Friction Stir Welding Behavior, *J. Eng. Manuf.*, 2010, **224**(8), p 1–16
7. M. Grujicic, G. Arakere, B. Pandurangan, A. Hariharan, C.-F. Yen, B.A. Cheeseman, and C. Fountzoulas, Statistical Analysis of High-Cycle Fatigue Behavior of Friction Stir Welded AA5083–H321, *J. Mater. Eng. Perform.*, 2010. doi:10.1007/s11665-010-9725-y
8. MIL-STD-1946A (MR), Welding of Aluminum Alloy Armor, Army Research Laboratory, Aberdeen Proving Ground, MD, 1989
9. W.B. Lee, C.Y. Lee, W.S. Chang, Y.M. Yeon, and S.B. Jung, Microstructural Investigation of Friction Stir Welded Pure Titanium, *Mater. Lett.*, 2005, **59**, p 3315–3318
10. W.M. Thomas and E.D. Nicholas, Friction Stir Welding for the Transportation Industries, *Mater. Des.*, 1997, **18**, p 269–273
11. J.Q. Su, T.W. Nelson, R. Mishra, and M. Mahoney, Microstructural Investigation of Friction Stir Welded 7050-T651 Aluminum, *Acta Mater.*, 2003, **51**, p 713–729
12. O. Frigaard, Ø. Grong, and O.T. Midling, A Process Model for Friction Stir Welding of Age Hardening Aluminum Alloys, *Metall. Mater. Trans. A*, 2001, **32**, p 1189–1200
13. M.W. Mahoney, C.G. Rhodes, J.G. Flintoff, R.A. Spurling, and W.H. Bingel, Properties of Friction-Stir-Welded 7075 T651 Aluminum, *Metall. Mater. Trans. A*, 1998, **29**, p 1955–1964
14. C.G. Rhodes, M.W. Mahoney, W.H. Bingel, R.A. Spurling, and C.C. Bampton, Effect of Friction Stir Welding on Microstructure of 7075 Aluminum, *Scripta Mater.*, 1997, **36**, p 69–75
15. G. Liu, L.E. Murr, C.S. Niou, J.C. McClure, and F.R. Vega, Microstructural Aspects of the Friction-Stir-Welding of 6061-T6 Aluminum, *Scripta Mater.*, 1997, **37**, p 355–361
16. K. Masaki, Y.S. Sato, M. Maeda, and H. Kokawa, Experimental Simulation of Recrystallized Microstructure in Friction Stir Welded Al Alloy Using a Plane-Strain Compression Test, *Scripta Mater.*, 2008, **58**, p 355–360
17. J.H. Cho, D.E. Boyce, and P.R. Dawson, Modeling Strain Hardening and Texture Evolution in Friction Stir Welding of Stainless Steel, *Mater. Sci. Eng. A*, 2005, **398**, p 146–163
18. M.F. Ashby, *Material Selection in Mechanical Design*, 3rd ed., Butterworth- Heinemann, Burlington, 2005
19. G.R. Johnson and W.H. Cook, A Constitutive Model and Data for Metals Subjected to Large Strains, High Strain Rates and High Temperatures, *Proceedings of the 7th International Symposium on Ballistics*, 1983
20. G.R. Johnson and W.H. Cook, Fracture Characteristics of Three Metals Subjected to Various Strains, Strain Rates and Temperatures, *Eng. Fract. Mech.*, 1985, **21**(1), p 31–48
21. R.E. Reed-Hill and R. Abbaschian, *Physical Metallurgy Principles*, 3rd ed., Brooks-Cole/Thomas Learning, Boston, MA, 1992
22. M. Grujicic, T. He, B. Pandurangan, W.C. Bell, N. Coutris, B.A. Cheeseman, W.N. Roy, and R.R. Skaggs, Development, Parameterization and Validation of a Visco-Plastic Material Model for Sand with Different Levels of Water Saturation, *J. Mater. Des. Appl.*, 2009, **223**, p 63–81
23. M. Grujicic, G. Arakere, H.K. Nallagatla, W.C. Bell, and I. Haque, Computational Investigation of Blast Survivability and Off-road Performance of an Up-armored High- Mobility Multi-purpose Wheeled Vehicle (HMMWV), *J. Automob. Eng.*, 2009, **223**, p 301–325
24. M. Grujicic, W.C. Bell, G. Arakere, and I. Haque, Finite Element Analysis of the Effect of Up-armoring on the Off-road Braking and Sharp-turn Performance of a High-Mobility Multi-purpose Wheeled Vehicle (HMMWV), *J. Automob. Eng.*, 2009, **223**(D11), p 1419–1434
25. A. Wenzel and J.M. Hennessey, Analysis and Measurements of the Response of Armor Plates to Land Mine Attacks, *Proceedings of the Army Symposium on Solid Mechanics*, Warren, Michigan, 1972, p 114–128
26. T. Hill and R. Westbrook, SWOT Analysis: It's Time for a Product Recall, *Long Range Plan.*, 1997, **30**(1), p 46–52